DOI: 10.1002/cbic.200800748

Discovery of Additional Members of the Tyrosine Aminomutase Enzyme Family and the Mutational Analysis of CmdF

Daniel Krug and Rolf Müller*[a]

The tyrosine aminomutase (TAM) CmdF converts L-Tyr preferentially to (R)-β-Tyr—a biosynthetic building block subsequently incorporated into the highly cytotoxic chondramides by the myxobacterium Chondromyces crocatus. *Together with the similar enzymes SgcC4 from* Streptomyces globisporus *and MdpC4 from* Actinomadura madurae, *which preferentially produce (S)-β-Tyr, CmdF belongs to a novel 2,3-aminomutase enzyme family closely related to the aromatic amino acid ammonia lyase. Although considerable insight into the underlying catalytic mechanism has been provided recently by structural and mechanistic studies, the key determinants of product specificity and stereochemical preference of TAM enzymes remain to be elucidated in detail. We report herein the discovery and heterologous expression of additional TAMs from prokaryotic sources. These studies reveal a high degree of evolutionary diversification within this expanding enzyme family. Attempts to genetically engineer CmdF to exhibit ammonia lyase-type activity by the exchange of conserved sequence motifs were largely unsuccessful. However, the variation of a semiconserved glutamic acid residue was found to impact stereoselectivity. Replacement of this residue by lysine significantly increased the enantiomeric excess of (R)-β-Tyr from 69 to 97% ee, while substitution with methionine promoted racemization. These results suggest that it should be possible to elucidate a mechanism for control of stereoselectivity in the TAM family by the application of directed evolution to CmdF. Furthermore, our findings indicate the potential to fine-tune the catalytic properties of TAMs for their use as biocatalysts or in engineered biosynthetic pathways.*

Introduction

β-Amino acids are building blocks in a variety of natural products exhibiting diverse structures and biological activities. For example, a β-tyrosine moiety is found in the highly cytotoxic chondramides produced by the myxobacterium *Chondromyces crocatus* and the structurally related antifungal jaspamides,[1–3] the enediyne antitumor antibiotics from *Streptomyces globisporus* and *Actinomadura madurae*,[4,5] and the potent bacterial protein biosynthesis inhibitor myxovalargin from *Myxococcus fulvus* (Scheme 1).[6] The molecular basis for the formation of chondramide and the enediynes has recently been studied in detail and has revealed the shared role of 2,3-aminomutases in both biosynthetic pathways.[4,7,8] The aminomutases show strong similarity to the ammonia lyase family, the members of which catalyze the elimination of ammonia from phenylalanine, tyrosine or histidine to yield an α,β-unsaturated acid.[9] Instead of releasing the resultant ammonia and α,β-unsaturated acid as free products, however, the aminomutases catalyze a subsequent 1,4-addition between the enzyme-bound intermediates to afford the β-amino acid as the end product. The catalytic electrophile in both cases is provided by the uncommon prosthetic group 4-methylideneimidazole-5-one (MIO), which results from the autocatalytic rearrangement of a signature Ala-Ser-Gly motif present in the protein.[10]

The exact role of MIO in ammonia lyase and aminomutase chemistry has been a matter of some controversy.[9,11] A number of studies on histidine ammonia lyase (HAL) and phenylalanine ammonia lyase (PAL) suggest the electrophilic attack of MIO on the ring of the aromatic substrate, which leads to the abstraction of a β proton followed by the elimination of ammonia.[9,12] However, data obtained from a recent mechanistic study on the tyrosine aminomutase (TAM), SgcC4, from the C-1027 enediyne biosynthetic pathway, support the proposed mechanism in which the reaction proceeds through the attack of MIO onto the substrate amine to generate a covalent adduct that promotes the α,β-elimination of ammonia from the amino acid.[11] In the ammonia lyase reaction pathway, the resulting *para*-hydroxycinnamic acid (*p*HCA) intermediate and free ammonia are released, while retention of ammonia in the active site of aminomutases facilitates readdition to the intermediate to yield the β-amino acid.[11] The facial selectivity of ammonia addition to *p*HCA results from the orientation of the intermediate in the binding pocket, and thus, in principle, both enantiomers of the β-amino acid product could result. Notably, the TAM enzymes SgcC4 and MdpC4 from the enediyne biosynthetic pathways have been demonstrated to produce preferentially (*S*)-β-Tyr,[5] while CmdF from *C. crocatus*

[a] *D. Krug, Prof. Dr. R. Müller*
Department of Pharmaceutical Biotechnology, Saarland University
P.O. Box 151150, 66041 Saarbrücken (Germany)
Fax: (+49) 681-302-70202
E-mail: rom@mx.uni-saarland.de

Supporting information for this article is available on the WWW under http://dx.doi.org/10.1002/cbic.200800748.

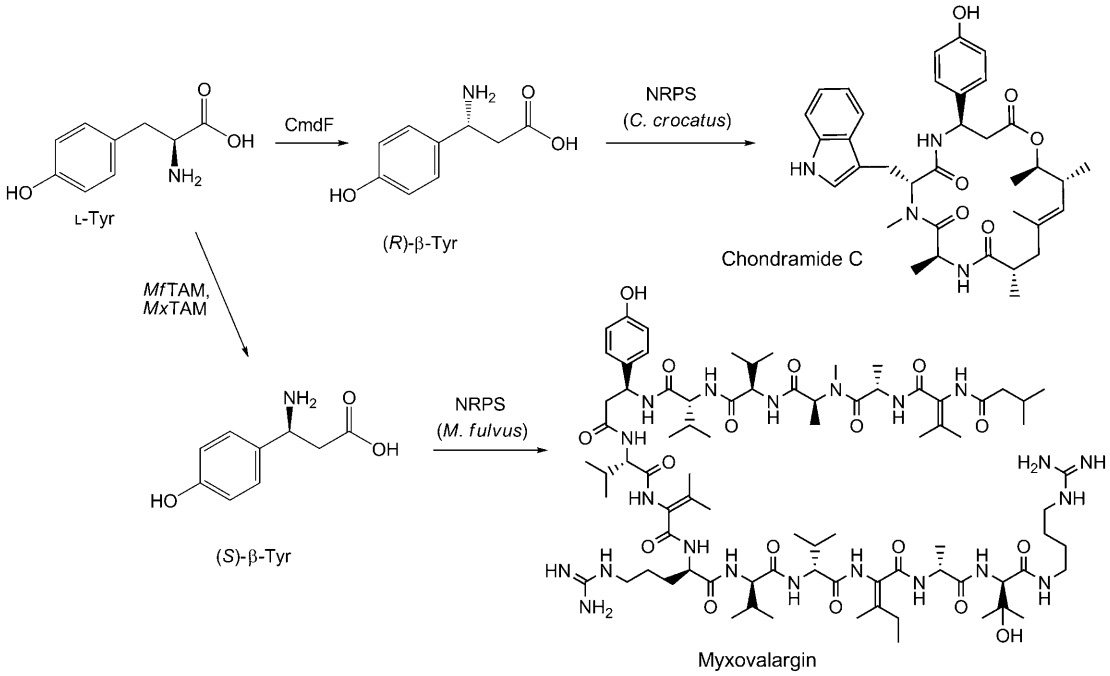

Scheme 1. The role of tyrosine aminomutases (TAMs) in the biosynthesis of two myxobacterial natural products. CmdF preferentially delivers (*R*)-β-Tyr, which is incorporated into the chondramides produced by *Chondromyces crocatus*, while *Mf*TAM and *Mx*TAM are proposed to produce (*S*)-β-Tyr, which is used in the biosynthesis of myxovalargin by *Myxococcus fulvus*.

primarily yields (*R*)-β-Tyr.[7] Furthermore, all of these enzymes exhibit tyrosine ammonia lyase (TAL) activity as a side reaction.

Enzymes of the ammonia lyase family have been extensively probed by site-directed mutagenesis in order to identify the structural determinants of their catalytic properties.[10,13–15] Key amino acids that control substrate selectivity have been reported recently for TAL from *Rhodobacter sphaeroides*.[16,17] A conserved His residue was found to direct substrate recognition; indeed, when the His was replaced by Phe, the enzyme exhibited efficient PAL activity; this identifies the His as a selectivity switch.[16] The recent analysis of the crystal structure of SgcC4 suggested the same role for the corresponding amino acid residue in TAMs.[11]

Enzymes of the TAM family have yet to be studied rigorously by these methods, and so the equivalent determinants of product specificity (i.e., what makes the enzymes aminomutases versus ammonia lyases) and stereoselectivity remain to be elucidated. Such information is a prerequisite for attempts to rationally manipulate the properties of aminomutases for various biotechnological applications. To provide a stronger basis for sequence comparison and phylogenetic analysis of aminomutases, we set out to extend the small TAM enzyme family by the identification of candidate genes from prokaryotic sources. Heterologous expression was carried out to enable biochemical characterization. We then used this information to attempt to manipulate the catalytic properties of the TAM, CmdF, from *C. crocatus* by site-directed mutagenesis.

Results and Discussion

Biochemical characteristics of the myxobacterial TAM, CmdF

We have previously investigated the role of CmdF in chondramide biosynthesis by targeted gene inactivation and confirmed that the recombinant enzyme directly converts L-Tyr to (*R*)-β-Tyr in vitro.[7] Like SgcC4, CmdF acts preferentially as an aminomutase rather than an ammonia lyase, as judged on the basis of the relative k_{cat} values for both reactions (Table 1). Alternative substrates were tested, but no measurable turnover with D-Tyr, Phe or His was observed. Monitoring a time course of the CmdF-catalyzed aminomutase reaction by HPLC-MS analysis revealed that (*R*)-β-Tyr is the kinetically preferred product, but that (*S*)-β-Tyr is also produced upon prolonged incubation

Table 1. Kinetic parameters for enzymes characterized in this study and comparison to the known aminomutase SgcC4.[3] Standard errors from a nonlinear regression analysis are given in parentheses.

Enzyme	Mutation[a]	K_M [μM]	k_{cat} [s^{-1}] (L-Tyr→β-Tyr)	k_{cat} [s^{-1}] (L-Tyr→*p*HCA)
CmdF	wt	377 (53)	7.2×10^{-3} (0.4×0^{-3})	0.5×10^{-3} (0.5×10^{-4})
*Cm*TAL	wt	348 (38)	0.9×10^{-3} (1×10^{-4})	0.011 (0.001)
SgcC4[b]	wt	28 (2)	0.01 (0.002)	1.2×10^{-3} (1×10^{-4})
$CmdF_{MIYMLV}$	62–67 (MIYMLV)	178 (23)	0.4×10^{-3} (0.2×10^{-4})	1.3×10^{-3} (0.6×10^{-4})

[a] Position of mutation (amino acid residues are given in parenthesis; numbering relates to CmdF); wt: wild-type enzyme. [b] Kinetic parameters as previously reported.[3] All other values originate from this study.

(Figure 1). This observation can be explained by the kinetically unfavorable conversion of Tyr to (*S*)-β-Tyr, but could also be partly due to the inherent racemase activity of CmdF, which

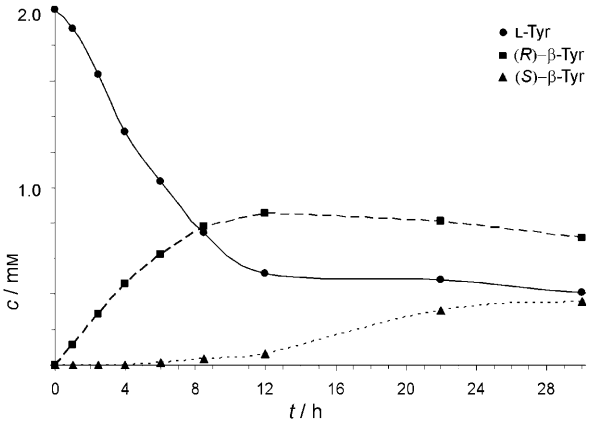

Figure 1. Time course for the in vitro conversion of L-Tyr→β-Tyr by the aminomutase, CmdF. The reaction was monitored by HPLC-MS analysis over a 30 h incubation period. ——●——: L-Tyr concentration; – – –■– – –: (*R*)-β-Tyr concentration; -----▲-----: (*S*)-β-Tyr concentration. Minor amounts of the substrate were also converted to *p*HCA because of ammonia lyase side activity (not shown).

has been demonstrated for SgcC4 before.[18] Both SgcC4 and CmdF exhibit relatively low catalytic efficiency in comparison with other characterized members of the ammonia lyase family.[9,10] However, high turnover numbers are probably not required to effectively furnish the natural product biosynthetic pathways in *S. globisporus* and *C. crocatus* with β-Tyr precursors, as the enzymes that typically accomplish secondary metabolite biosynthesis are themselves rather slow.[19]

The preferential production of opposite β-Tyr enantiomers constitutes a striking difference between CmdF and the other two biochemically characterized aminomutase enzymes, SgcC4 from *S. globisporus* and MdpC4 from *A. madurae*.[5,7,18] It has been proposed that this stereochemical differentiation results from the attack of the amine-MIO adduct on opposite faces of the *trans*-cinnamate intermediate. Indeed, a recent structural study of SgcC4 bound to an inhibitor showed that the active site could accommodate different substrate orientations while maintaining the key interactions between the substrate and active-site residues necessary to achieve catalysis.[11] On the basis of this model, it seems likely that further amino acids in proximity to the active site help to orient the substrate, even if their role might not be obvious from existing crystallographic data. The availability of a reasonable number of representative sequences is an important prerequisite for investigating such potentially subtle determinants of substrate selectivity, product specificity or stereoselectivity. As a first step towards enabling more robust comparisons, we aimed to identify and characterize further aminomutase candidates from prokaryotic sources.

Cloning and characterization of additional TAMs

A search for putative homologues of CmdF in public databases yielded a large number of similar protein sequences from diverse microbial sources, the vast majority of which had been annotated as HAL enzymes in the course of genome sequencing projects. The deduced amino acid sequence of Rmet_0231 from *Cupriavidus metallidurans* displayed a high degree of similarity to CmdF (43% identity/58% similarity) as well as to SgcC4 (54/69%) and MdpC4 (56/68%); Rmet_0231 was also found to be highly similar to many putative HAL sequences (up to 42% identity/60% similarity to HutH from *Bacillus* spp.). However, Rmet_0231 lacks a conserved glutamic acid residue shown to be characteristic of HALs (i.e., Glu414 in *Pp*HAL,[10] position 431 in the alignment in Figure 2), and the surrounding region closely resembles the sequence motif found in the TAM proteins and *Rc*TAL (NQD(V/I)VSMG, position 430–437 in CmdF, Figure 2). Therefore, we suspected that Rmet_0231 might encode an unrecognized member of the TAL/TAM family. The gene was cloned from the genomic DNA of *Cv. metallidurans* and the corresponding protein (later named *Cm*TAL) was overexpressed in *E. coli* BL21 as a C-terminal fusion with glutathione *S*-transferase (GST), as described previously for CmdF.[7] The purification of *Cm*TAL (532 aa, calculated $M_W = 56029$ Da) was carried out by glutathione affinity chromatography, followed by on-column cleavage with the PreScission protease. The purified enzyme was then incubated with L-Tyr, L-Phe and L-His in order to assay for both ammonia lyase and aminomutase activity. HPLC-diode array detector (DAD) MS analysis revealed unambiguously that *Cm*TAL produces *p*HCA and β-Tyr, in vitro, to preferentially yield the *R* enantiomer, as observed for CmdF. The kinetic characterization (relative k_{cat}) revealed that *Cm*TAL is more efficient as a TAL than it is as a TAM (Figure 3, Figure 4F and Table 1). No turnover was observed with either Phe or His. The physiological relevance of the TAL and TAM activity exhibited by *Cm*TAL is at present unknown, as the in silico analysis of the sequenced chromosomes and plasmids of *Cv. metallidurans* CH34 did not reveal typical genes encoding nonribosomal peptide synthetases, which might use a β-Tyr building block for secondary metabolite biosynthesis. In addition, no homologue of a gene encoding the prokaryotic photoactive yellow protein (Pyp), which requires *p*HCA as a covalently attached cofactor,[20] could be identified.

The successful biochemical characterization of *Cm*TAL indicated that proteins that display overall sequence similarity to HAL and exhibit the aforementioned "TAL/TAM-like" sequence motif could be novel members of the TAL/TAM family. We reasoned that these sequence properties could serve as a guide for the cloning of further aminomutase genes from unsequenced microbial genomes, and help to discriminate against the widely abundant HAL-encoding sequences. *Myxococcus fulvus* f65 was anticipated to be a source of an aminomutase-encoding gene as this strain produces myxovalargin A—a known inhibitor of bacterial protein biosynthesis that contains a β-Tyr moiety.[6,21] The configuration of this building block was determined by HPLC-MS following hydrolysis of myxovalargin and its chiral derivatization (Figure 5). This analysis revealed un-

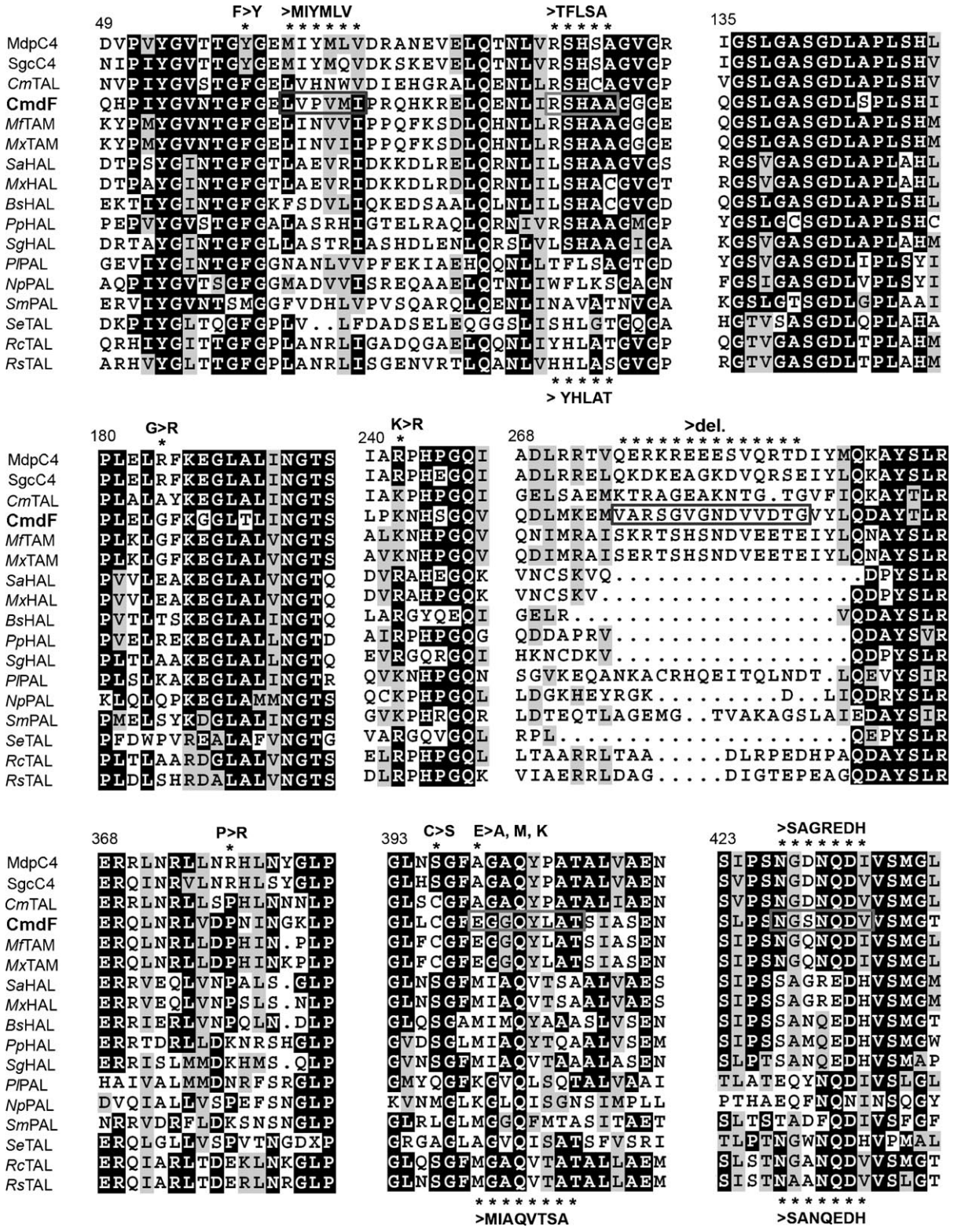

Figure 2. A portion of an amino acid alignment of known TAMs and ammonia lyases exhibiting substrate specificity for Tyr, Phe and His. The ClustalW algorithm was used for full-length alignment, and the included sequences are from the following sources (protein name, accession number and length in amino acids (aa) are given in parentheses): *Actinomadura madurae* (MdpC4, ABY66005, 537 aa), *Streptomyces globisporus* (SgcC4, AAL06680, 539 aa), *Cupriavidus metallidurans* (*Cm*TAL, Rmet_0231, ABF07117, 533 aa), *Chondromyces crocatus* (CmdF, AM179409, 531 aa), *Myxococcus fulvus* (*Mf*TAM, FM212243, 527 aa), *Myxococcus* sp. (*Mx*TAM, FM212244, 527 aa), *Stigmatella aurantiaca* (*Sa*HAL, AAK57183, 510 aa), *Myxococcus xanthus* (*Mx*HAL, MXAN_3465, ABF90953, 508 aa), *Bacillus subtilis* (*Bs*HAL, HutH, BAA06644, 508 aa), *Pseudomonas putida* (*Pp*HAL, HutH, P21310, 510 aa), *Streptomyces griseus* (*Sg*HAL, HutH, P24221, 514 aa), *Photorhabdus luminescens* (*Pl*PAL, StlA, CAE14527, 532 aa), *Nostoc punctiforme* (*Np*PAL, Npun_R2068, YP_001865631, 569 aa), *Streptomyces maritimus* (*Sm*PAL, EncP, AAF81735, 523 aa), *Saccharothrix espanaensis* (*Se*TAL, Sam8, ABC88669, 510 aa), *Rhodobacter capsulatus* (*Rc*TAL, RRC01844, 531 aa) and *Rhodobacter sphaeroides* (*Rs*TAL, YP_355075, 523 aa). Regions chosen for mutagenesis in this study are indicated above and below the sequences (see the main text for details). Amino acid residue numbering relates to CmdF.

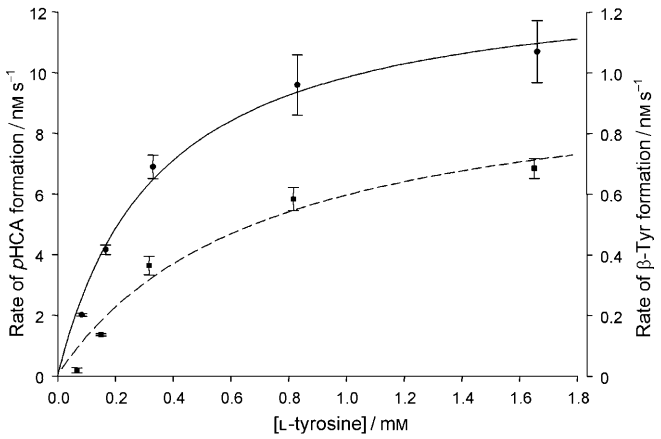

Figure 3. Michaelis–Menten plot obtained by direct nonlinear regression for TAL (——●——; left *y* axis) and TAM (– – –■– – –; right *y* axis) activity exhibited by recombinant *Cm*TAL. Notably, the aminomutase activity exhibited by *Cm*TAL distinguishes this enzyme from other TALs, which do not usually display additional aminomutase activity (e.g., *Se*TAL from *S. espanaensis*).[21]

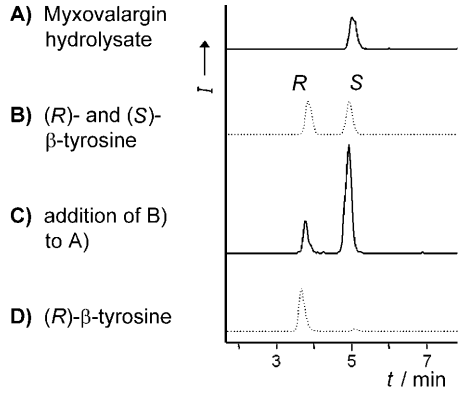

Figure 5. A) HPLC-MS analysis of a myxovalargin hydrolysate after chiral derivatization revealed that myxovalargin exclusively contains (*S*)-β-Tyr. B) A mixture of both β-Tyr enantiomers. C) A myxovalargin hydrolysate applied with a mixture of both β-Tyr enantiomers. D) Derivatized, commercially available, (*R*)-β-Tyr reference substance. The extracted-ion chromatograms are shown (*I*, intensity).

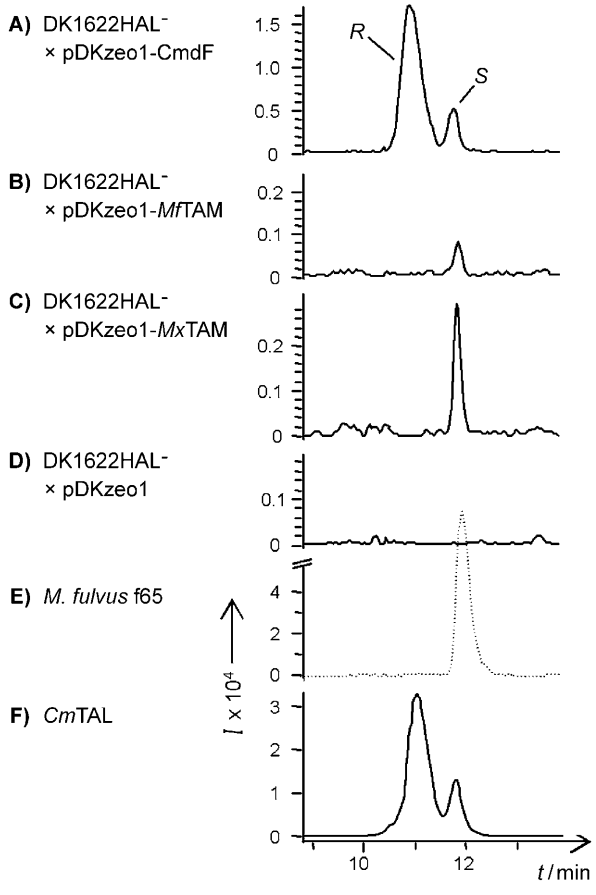

Figure 4. Production of β-Tyr by aminomutase enzymes investigated in this study and the analysis of stereochemistry in vivo and in vitro. Culture supernatants from mutant strain *M. xanthus* DK1622HAL⁻, transformed with expression constructs: A) pDKzeo1-CmdF, B) pDKzeo1-*Mf*TAM, C) pDKzeo1-*Mx*TAM, and D) plasmid pDKzeo1 (negative control) were analyzed by HPLC-MS following chiral derivatization. E) Identification of (*S*)-β-Tyr in culture supernatants from the myxovalargin-producing strain *Myxococcus fulvus* Mx f65. F) Activity assay of recombinant *Cm*TAL in vitro. Extracted-ion chromatograms are shown and the signals at retention times of 11 and 12 min correspond to (*R*)- and (*S*)-β-Tyr, respectively. Scales on the *y* axes were adjusted to account for varying signal intensities (*I*) between experiments.

ambiguously that only (*S*)-β-Tyr is incorporated into myxovalargin A, in contrast to the exclusive use of (*R*)-β-Tyr in the biosynthesis of the chondramides.[7] We anticipated that the identification of a second myxobacterial aminomutase, which preferentially generates (*S*)-β-Tyr, could facilitate the identification of stereochemical determinants in the aminomutase family. Therefore, we aimed to characterize biochemically the putative aminomutase from *Myxococcus*.

Degenerate primers TAM-ASGDL and TAM-NQDVV were derived from the DNA sequence of CmdF (Table S1 in the Supporting Information) and used for the PCR amplification of a 902 bp fragment from the genomic DNA of *M. fulvus* f65; the resulting sequence showed convincing similarity to CmdF. Employing the arbitrary PCR technique as previously described,[22] the initial sequence was extended towards the putative start and stop codons. Once the complete sequence was in hand, primers TAMf65-start and TAMf65-stop were used to clone the complete *Mf*TAM gene (1581 bp). The same primer pair was subsequently used to amplify a homologous sequence from another myxovalargin-producing myxobacterium, the *Myxococcus* sp. isolate Mx-B0. Both *Mf*TAM and *Mx*TAM exhibit high similarity to CmdF on the amino acid level (59% identity, 70% similarity) and were cloned into the pGEX-6P-1 vector for heterologous expression as a C-terminal translational fusion with GST. Unfortunately, the resulting recombinant proteins were insoluble and recloning into a variety of available *E. coli* expression systems did not afford soluble protein (data not shown).

To overcome this obstacle, *M. xanthus* DK1622 was utilized as a host for the heterologous expression of *Mf*TAM and *Mx*TAM. Expression plasmids were constructed based on the pDKzeo1 vector, which enables integration into the *M. xanthus* DK1622 chromosome via the *attB* phage attachment site. The plasmids also contained a zeocin-resistance cassette and a single copy of the cloned gene under the control of the constitutive T7A1 promoter.[23] In order to allow for the detection of alternative HAL activity, the chromosomal *hutH*-homologue MXAN_3465 was inactivated in *M. xanthus* DK1622. This open

reading frame represents the only gene encoding a protein with significant similarity to ammonia lyases in the DK1622 genome (*Mx*HAL, 49% identity/66% similarity to the HAL HutH from *Bacillus* spp.). Its inactivation was achieved by the standard method of plasmid insertion mediated through single-crossover homologous recombination. GC-MS analysis confirmed that the resulting kanamycin-resistant expression strain DK1622HAL$^-$ no longer produced urocanic acid—the usual product of HAL-catalyzed ammonia elimination from His.

The supernatants from cultures of DK1622HAL$^-$ transformed with expression plasmids pDKzeo1-CmdF, pDKzeo1-*Mf*TAM, pDKzeo1-*Mx*TAM, and pDKzeo1 (without insert, negative control) were analyzed for the production of β-Tyr by HPLC-MS, following chiral derivatization. This analysis revealed that the DK1622HAL$^-$ strain expressing CmdF produced predominantly (*R*)-β-Tyr (Figure 4, trace A), while exclusively (*S*)-β-Tyr was detected in cultures of DK1622HAL$^-$ expressing either *Mf*TAM or *Mx*TAM (Figure 4, traces B and C). Thus, *Mf*TAM and *Mx*TAM exhibit aminomutase activity and stereoselectivity in vivo consistent with their predicted role in supplying (*S*)-β-Tyr for myxovalargin biosynthesis by *M. fulvus* f65 (Figure 4, trace E). Efforts are currently underway to establish a method for the genetic manipulation of this strain in order to confirm the proposed role of *Mf*TAM by targeted gene inactivation. Only trace amounts of *p*HCA were identified in supernatants from DK1622HAL$^-$ expressing *Mf*TAM and *Mx*TAM, and neither cinnamic acid nor urocanic acid were detected by GC-MS analysis (data not shown); this suggests that these enzymes do not exhibit primarily TAL, PAL or HAL activity.

Effects of ammonia lyase/aminomutase-like mutations on the function of CmdF

As structural data only exist for the aminomutase SgcC4, and attempts to crystallize CmdF were so far not successful, we aimed to use primary sequence comparison and the results of earlier biochemical and structural studies[9,11,16,24–26] to guide our efforts to modulate the catalytic properties of CmdF by site-directed mutagenesis. CmdF was the logical choice for these experiments, due to its favorable expression in *E. coli* and its pronounced preference for (*R*)-β-Tyr formation. A number of CmdF variants were generated with an overlap extension PCR strategy (see the Experimental Section), and mutant enzymes were purified and assayed for aminomutase and ammonia lyase activity by using the substrates L-Tyr, L-Phe and L-His.

The changes made to the CmdF amino acid sequence are detailed in Table 2 and indicated in Figure 2 (see also Tables S2 and S3). Briefly, certain conserved sequence motifs found in enzymes of the ammonia lyase family were transferred to the corresponding positions in CmdF, with the expectation that the mutant CmdF enzymes might exhibit altered product specificity and/or substrate selectivity. Unfortunately, most mutations proved to be detrimental to CmdF and yielded inactive enzyme with no measurable aminomutase or ammonia lyase activity with any of the tested substrates, even after prolonged incubation (Table 2 A). This loss of function can be explained, at least in some cases, by the loss of key residues with an established role in the catalytic mechanism. Alterations in the primary sequence might also have interfered with the proper folding of the proteins, which is particularly likely for the $CmdF_{del}$ mutant lacking a stretch of sequence. In general, the TAM structure does not seem to readily tolerate the introduction of conserved motifs from members of the HAL, PAL or TAL family. $CmdF_{MIYMLV}$ was the only mutant that still acted as an efficient aminomutase and ammonia lyase with the substrate L-Tyr—albeit with a significant shift from aminomutase towards ammonia lyase activity, as suggested by the relative k_{cat} values (Table 1). However, the stretch of sequence introduced in this mutant was not derived from an ammonia lyase protein, but

Table 2. Rates of β-Tyr formation (v_{rel}) for CmdF variants, relative to the wild-type enzyme, determined at an L-Tyr concentration of 1.8 mM (standard deviations in parentheses; n.d.: not detectable). A) Multiresidue mutations, and B) single amino acid substitutions were carried out.

Enzyme	Position[a]	Mutation[b]	$v_{rel.}$[c]	Explanation
A)				
$CmdF_{TFLSA}$	81–85: RSHAA	TFLSA	n.d.	PAL (FL)–TAL (HL) substrate selectivity switch;[16] (SH) conserved in HAL and TAM
$CmdF_{YHLAT}$	"	YHLAT	n.d.	
$CmdF_{SAGREDH}$	427–433: NGSNQDV	SAGREDH	n.d.	TAM/TAL motif around Q431, strictly-conserved E431 in HAL enzymes[24]
$CmdF_{SANQEDH}$	"	SANQEDH	n.d.	
$CmdF_{del.}$	275–288	deleted	n.d.	Deletion of 14 aa from "outer loop" region[25]
$CmdF_{MIAQVTSA}$	399–406: EGGQYLAT	MIAQVTSA	0.012 (0.002)	Introduction of HAL-like motif including V403[11]
$CmdF_{MIYMLV}$	62–67: LVPVMI	MIYMLV	[d]	Aminomutase-like sequence exchange
B)				
$CmdF_{F59Y}$	59: F	Y	0.8 (0.1)	Single amino acid alteration
$CmdF_{G184R}$	184: G	R	2.4 (0.3)	"
$CmdF_{K242R}$	242: K	R	1.7 (0.3)	"
$CmdF_{P377R}$	377: P	R	1.1 (0.2)	"
$CmdF_{C396S}$	396: C	S	1.2 (0.2)	"

[a] Position and original CmdF sequence mutated. Underlined amino acid residues are referred to in the explanation. [b] Mutation introduced into the CmdF sequence; see also Figure 2. [c] Relative rate of L-Tyr→β-Tyr conversion, compared to that of the wild-type CmdF. [d] See the kinetic parameters in Table 1.

from the aminomutase MdpC4, which (together with SgcC4) differs markedly from CmdF and the other aminomutase enzymes in this sequence region (Figure 2).

In addition to the multiresidue mutations, a number of single-residue amino acid substitutions were also performed (Table 2 A). The positions chosen for these mutations are differentially conserved among aminomutase and ammonia lyase representatives (Figure 2), but have not been assigned specific roles through structural studies. These point mutations yielded mostly TAM enzymes that exhibited only minor differences in catalytic efficiency, as judged by the relative velocities of product formation (Table 2 B), despite the fact that some of these amino acids significantly altered the chemical properties and/or steric requirements of the side chains. Thus, the CmdF structure can accommodate site-specific alterations in semiconserved positions, and essentially retain its original enzymatic functionality.

Table 3. Relative rate of formation (v_{rel}) and enantiomeric excess (%*ee*) of (*R*)-β-Tyr as determined by HPLC-MS analysis of CmdF and mutant enzymes $CmdF_{E399A}$, $CmdF_{E399M}$, $CmdF_{E399K}$. The values in parentheses are standard deviations.

Enzyme[a]	$v_{rel.}$ L-Tyr→β-Tyr	%*ee* of (*R*)-β-Tyr	$v_{rel.}$ L-Tyr→*p*HCA
CmdF, wt	1	69 (1.5)	1
$CmdF_{E399A}$	0.7 (0.12)	59 (2.1)	2.25 (0.3)
$CmdF_{E399M}$	0.08 (0.02)	12 (1.3)	0.65 (0.09)
$CmdF_{E399K}$	0.08 (0.01)	97 (1.2)	0.4 (0.08)

[a] Subscript letters and numbers denote mutations and their position; wt: wild-type enzyme.

Variation of Glu399 influences the stereoselectivity exhibited by CmdF

The glutamic acid residue at position 399 in CmdF is strictly conserved in the three myxobacterial aminomutases, but the corresponding position is occupied by alanine in SgcC4, MdpC4 and *Cm*TAL (Figure 2). HAL enzymes almost invariably carry a methionine at this position, while lysine is found in most PALs.[24] This semiconserved amino acid residue has been assigned a substrate-directing function on the basis of a crystallographic study on a PAL from *Rhodosporidium toruloides*.[24] Although the recent structural analysis of SgcC4 bound to an inhibitor did not suggest a specific role for the corresponding residue, it is located in close proximity to Tyr403, which has been implicated in substrate binding.[11] To explore this issue, we evaluated the impact of three mutations—E399A, E399M and E399K—on the catalytic properties of CmdF. The rate of β-Tyr formation by $CmdF_{E399A}$ was comparable to that of the wild-type enzyme but was significantly reduced for the E399M and E399K variants (Table 3). The stereoselectivity of the latter two enzymes also differed markedly from that of the wild-type; $CmdF_{E399M}$ exhibited increased product racemization, while $CmdF_{E399K}$ produced a higher enantiomeric excess of (*R*)-β-Tyr even upon prolonged incubation (Figure 6 and Table 3). Thus, the residue at position 399 in CmdF strongly influences the facial preference for the addition of ammonia to either face of the planar *p*HCA intermediate in the course of the aminomutase reaction. Stereoselectivity is likely to be accomplished by directing the Tyr substrate in the binding pocket to a suitable orientation. As the amino acid at position 399 does not strictly correlate with aminomutase stereoselectivity, it must be only one of several key residues that modulate the structural framework of the active site. A crystallographic inves-

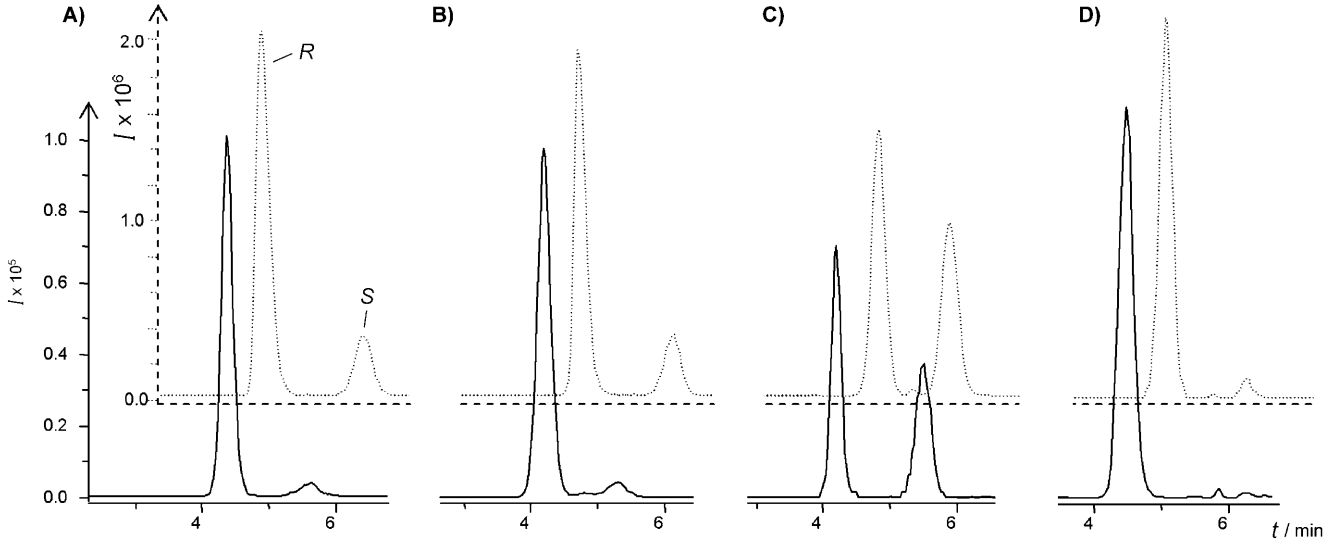

Figure 6. Analysis of β-Tyr product stereochemistry after incubation of CmdF enzyme variants with L-Tyr. A) Wild-type enzyme, B) mutant $CmdF_{E399A}$, C) mutant $CmdF_{E399M}$, D) mutant $CmdF_{E399K}$. The signal at 4.2 min corresponds to (*R*)-β-Tyr, while that at 5.6 min represents (*S*)-β-Tyr. Extracted-ion chromatograms from the HPLC-MS analysis following chiral derivatization are shown (*I*, intensity). Samples were taken at time points corresponding to comparable substrate turnover. Chromatograms in the foreground (——) represent early measurements, while those in the background (····) represent measurements after prolonged incubation.

tigation of CmdF and its variants with altered stereoselectivity bound to an inhibitor,[11] should reveal further stereochemical determinants in the TAM family.

The TAMs constitute an evolutionarily diversified enzyme family

Including the newly characterized TAM proteins, the TAM enzyme family now comprises six representatives, which differ markedly with respect to product stereospecificity and relative preference for aminomutase to ammonia lyase activity, while sharing the same strict substrate specificity for L-Tyr. We aligned the sequences of the six TAM enzymes with prokaryotic proteins with confirmed HAL, PAL, and TAL activity, using the ClustalW algorithm (Figures 2 and 7).[5,10,14,15,18,20,27,28] The following picture emerges from this comparison: 1) the TAMs uniformly share a higher degree of sequence conservation with HALs than with TALs or PALs; this supports our hypothesis that, contrary to expectation, they might not constitute a side-branch of the TAL group, but instead could have coevolved from an early "HAL-like" ancestor, and 2) no clustering according to stereoselectivity occurs within the TAM family, and the observed grouping instead reflects underlying phylogenetic relationships. Taken together, these data suggest that characteristic traits of the aminomutases, such as their product stereoselectivity, have evolved independently in distant phylogenetic clades, that is, they are polyphyletic.

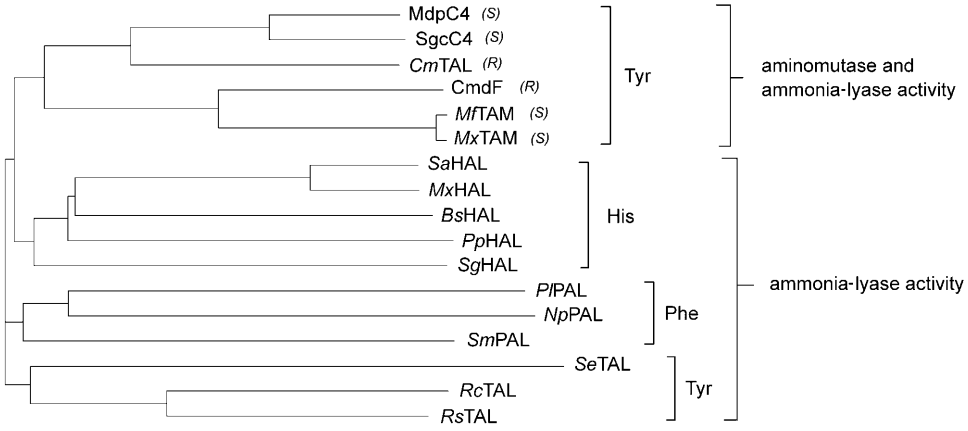

Figure 7. Similarity of proteins with confirmed TAM and/or TAL, PAL or HAL activity from various bacterial sources. The grouping pattern reflects substrate preference (Tyr, Phe or His) and product specificity, but not the stereoselectivity of enzymes capable of acting as aminomutases; (*R*) and (*S*) indicate the preferred aminomutase product stereochemistry. The neighbor-joining method was used for tree construction. Accession numbers and additional information for the enzymes involved are given in the legend of Figure 2.

TAMs have now been reported from bacterial lineages as distant as β-proteobacteria, δ-proteobacteria and actinomycetales, and in all instances, the preferred product stereospecificity matches the configuration of a chiral building block found in a secondary metabolite from the respective strain (except for *Cv. metallidurans*, from which, to the best of our knowledge, no β-Tyr-containing natural product has been identified to date). Thus, convergent evolution from a common ammonia lyase ancestor might have taken place. The catalytic properties of each individual TAM enzyme seem to have evolved in order to furnish a specific biosynthetic pathway with a β-Tyr building block. The detailed amino acid mutations that achieve this "fine tuning" might not necessarily be conserved in proteins that exhibit the same characteristics,[29] a feature which could significantly impede efforts to deduce the conserved motifs responsible for specific catalytic properties. Indeed, comparison of the sequences of Mdp4, SgcC4, *Mf*TAM, *Mx*TAM, CmdF and *Cm*TAL did not yield predictable sequence motifs that correlate with stereochemical preference.

Conclusions

The data reported here support a high degree of evolutionary diversification within the expanded TAM enzyme family; this suggests that family members were acquired by convergent evolution. Site-directed mutagenesis of CmdF revealed the relative inflexibility of the scaffold towards efforts to convert it towards ammonia lyase-like activity. However, alteration in stereoselectivity could be obtained by the mutagenesis of a single amino acid. Future studies—perhaps based on sequence-swapping or directed evolution techniques—should help to further illuminate the molecular basis for the control of product stereospecificity in this enzyme family. Nonetheless, our finding that a single residue modulates stereocontrol indicates that it might be possible to tailor the catalytic properties of TAMs to increase their potential as highly stereoselective biocatalysts. In the future, they might also be of use for the supply of chiral β-Tyr building blocks in designed biosynthetic pathways.

Experimental Section

Chemicals, media, strains and fermentation conditions: All chemicals were purchased from Sigma–Aldrich unless indicated otherwise. *E. coli* strain DH10B was grown at 37 °C, and strain BL21 was grown at 30 °C in Erlenmeyer flasks in liquid LB medium, supplemented with the following antibiotics whenever appropriate: ampicillin (100 μg mL^{-1}), kanamycin sulfate (50 μg mL^{-1}), carbenicillin (100 μg mL^{-1}) and zeocin (25 μg mL^{-1}). *Myxococcus xanthus* DK1622 and its descendants were grown in liquid CTT medium (30 °C, 200 rpm) and maintained on CTT agar plates[30] containing kanamycin sulfate (40 μg mL^{-1}) and zeocin (20 μg mL^{-1}), when required for selection. The sequences of primers as well as plasmid maps can be found in the Supporting Information (Tables S1–S3 and Figure S1).

Recombinant production, purification and activity assay of aminomutase proteins: The heterologous expression of aminomutase

proteins as C-terminal fusions to GST was performed with a method similar to that described previously.[7] Briefly, *E. coli* BL21, carrying a pGEX-derived expression plasmid, was grown, overnight, in LB medium (2 mL) with ampicillin and was inoculated at a 1:100 dilution into LB medium (50 mL) containing carbenicillin. When growth reached an OD_{600} of 1.0, IPTG was added (final concentration 0.4 mM) and incubation was continued (2 h, 30 °C). Cells were harvested by centrifugation, resuspended in PBS buffer and passed twice through a French press cell. The crude lysate was clarified by centrifugation, and protein purification was carried out by affinity chromatography with GST-Sepharose. The GST tag was cleaved by using the PreScission Protease according to manufacturer recommendations (4 °C) and the purified protein was eluted in buffer containing Tris (50 mM, pH 7.0), NaCl (150 mM), EDTA (1 mM) and dithiothreitol (1 mM).

Enzyme activity was assayed by using purified protein (10–50 μg) in Tris buffer (0.1 mM, pH 8.8, 30 °C) with substrate concentrations ranging from 50 μM–1.8 mM of L-Tyr or up to 10 mM of Phe or His. To investigate the formation of β-Tyr, aliquots from the assays were derivatized with *O*-phthaldialdehyde-*N*-acetyl-cysteine (OPA-NAC) reagent and directly submitted to HPLC analysis.[31] The separation of the diastereomeric β-Tyr derivatives was achieved on a Synergi HydroRP C18 column (100×2 mm, 2.5 μm particle size; Phenomenex, Germany) with a mobile phase system as described previously.[27] The Agilent 1100 series solvent delivery system was coupled to an ESI-MS Bruker HCTplus mass spectrometer operating in manual MS/MS mode by using positive ionization. OPA-NAC derivatives of β-Tyr were identified and quantified by their characteristic fragment ions (*m/z* 314, 279 and 150, generated from the monoprotonated parent ion of *m/z* $[\beta\text{-Tyr+OPA-NAC+H}]^+ = 443$). The formation of *p*HCA and urocanic acid was monitored by DAD-coupled HPLC (detection at 310 and 280 nm, respectively). For the determination of kinetic parameters, initial velocities of product formation were fit to the Michaelis–Menten equation by direct nonlinear regression by using the enzyme kinetics module of the SigmaPlot software suite (Systat Software Inc., San Jose, CA, USA). All calculations are based on measurements from at least three independent experiments.

Determination of the configuration of β-Tyr in myxovalargin: Myxovalargin A (0.5 mg) was hydrolyzed in HCl (1 mL, 6 N, 99 °C, 12 h). The solvent was removed by evaporation and borate buffer (100 μL, 0.4 M, pH 10.2) was added to the solid residue. The suspension was clarified by centrifugation and used for OPA-NAC derivatization followed by HPLC-MS analysis as described above.

Cloning of the gene encoding *Cm*TAL from *Cupriavidus metallidurans*: Cells were harvested from a liquid culture of strain *Cv. metallidurans* CH34 (DSM No. 2839) by centrifugation,[32] and chromosomal DNA was prepared by using the Gentra Puregene Kit (Qiagen) according to manufacturer's recommendations. PCR amplification of a 1602 bp fragment encoding the gene Rmet_0231 was performed by using Phusion Polymerase (Finnzymes, Espoo, Finland). Primers Cme231-start and Cme231-stop were used to introduce BamHI and EcoRV restriction sites at the 5′ and 3′ ends of the coding sequence, respectively. The plasmid was digested with both enzymes, the fragment was inserted into the BamHI/EcoRV-digested pGEX-6P-1 vector by using T4 DNA ligase (MBI-Fermentas) and the resulting construct (pGEX6p-*Cm*TAL) was transferred into *E. coli* DH10B by electroporation. The fidelity of the PCR amplification was verified by sequencing of the plasmid DNA (MWG Eurofins, Ebersberg, Germany), which was prepared with the GeneJet plasmid isolation kit (MBI-Fermentas).

Cloning of genes encoding *Mf*TAM from *Myxococcus fulvus* f65 and *Mx*TAM from *Myxococcus* Mx-B0: The degenerate primer pair TAM-ASDGL1 and TAM-NQDVV1 was employed for the PCR amplification of a 902 bp fragment from the genomic DNA of strain *M. fulvus* f65 by using Taq polymerase (MBI-Fermentas). The fragment was cloned into the pCR2.1Topo vector (Invitrogen) and sequenced. Multiple rounds of arbitrary PCR were subsequently carried out to extend the sequence information up- and downstream of the cloned fragment,[22] and primers TAMF65-start and TAMF65-stop were used for the final PCR amplification of the 1581 bp *Mf*TAM coding sequence by using Phusion polymerase, which added mutagenic BglII and EcoRI restriction sites. The same primer pair was also used to amplify a fragment of the same size from the genomic DNA of the *Myxoccous* sp. isolate Mx-B0 (R. Garcia and S. Werner, unpublished). The PCR fragments were cloned into the pJET1/blunt vector (MBI-Fermentas), which was then transformed into *E. coli* DH10B. Plasmid DNA was prepared from pJET-*Mf*TAM and pJET-*Mx*TAM, and the insert sequences were determined by sequencing. The fragments were excised from the pJET1-derived plasmids by using restriction enzymes BglII and EcoRI and ligated into the BamHI/EcoRI-digested pGEX-6P-1 vector to yield the expression constructs pGEX-*Mf*TAM and pGEX-*Mx*TAM, respectively.

Inactivation of the *hutH* homologue (*MxHAL*) in *M. xanthus* DK1622: An internal 592 bp fragment of the gene MXAN_3465 was amplified from genomic DNA by using Taq polymerase and primers HAL1622fwd1 and HAL1622rev1 and cloned into the pCR2.1Topo vector. The resulting inactivation plasmid (pTOPO-1622HAL) was used for the electroporation of *M. xanthus* DK1622 as previously described,[33] and viable colonies were obtained on CTT agar supplemented with kanamycin. The integration of the plasmid into the MXAN_3465 locus was verified by PCR with primers 1622con1 and 1622con2, which are located outside the amplified region, in combination with vector-specific primers pTOPOin and pTOPOout. To confirm the absence of urocanic acid in supernatants of the resulting DK1622-HAL$^-$ mutant cultures, an aliquot from the medium was clarified by centrifugation and subjected to HPLC fractionation. Fractions corresponding to the retention time range for urocanic acid ($t_R \approx 1.5$ min) were collected following chromatography on a Synergi FusionRP C18 column (150×2 mm, 4 μm particle size; Phenomenex) under isocratic conditions (mobile phase consisting of 20 mM ammonium formate in 0.5% aqueous MeOH, flow-rate of 0.4 mL min^{-1}) the samples were evaporated to complete dryness (60 °C), and then the residue was derivatized with *N*-methyl-*N*-(trimethylsilyl)trifluoroacetamide (MSTFA) prior to GC-MS analysis.

Construction of pDKzeo1-based plasmids for expression in the *M. xanthus* DK1622-HAL$^-$ mutant: Plasmid pDKzeo1 is a derivative of the plasmid pCK_T7AI_att for integration into the *Myxococcus* chromosome via the *attB* phage attachment site,[23] but it lacks the kanamycin- and ampicillin-resistance genes. The plasmid was obtained by PCR amplification of a 4975 bp fragment from pCK_T7AI_att with Phusion polymerase and primers pCKSnaB1 and pCKBglII, followed by the phosphorylation of the blunt-ended PCR product, self-ligation with T4 DNA-ligase and transformation into *E. coli* DH10B. Plasmid pDKzeo1 was digested with BamHI and EcoRI in order to ligate the vector backbone with the coding sequences for CmdF, *Mf*TAM and *Mx*TAM, excised from the respective precursor plasmids with EcoRI and either BamHI or BglII, to create compatible ends. The resulting plasmids pDKzeo1-CmdF, pDKzeo1-*Mf*TAM and pDKzeo1-*Mx*TAM contained the cloned inserts in-frame with an ATG start codon preceded by a ribosome-binding site and the T7AI promoter.[23] The plasmids were used for the transforma-

tion of *M. xanthus* DK1622-HAL$^-$ according to the standard protocol,[33] followed by selection on CTT agar containing both kanamycin and zeocin. Colonies were obtained after 5–7 days of incubation, and integration into the chromosome was verified by using a PCR strategy, with primers zeo_for and zeo_rev (specific for the zeocin-resistance gene) as well as primers specific for the cloned aminomutase sequences. Recombinant strains were grown in liquid CTT medium (10 mL) supplemented with kanamycin and zeocin for four days (30 °C, 200 rpm). Sample aliquots were taken, clarified by centrifugation and treated further depending on the intended analysis. For the analysis of *p*HCA content by HPLC, the samples were acidified with acetic acid (10%, *v/v*), extracted with ethyl acetate, dried and redissolved in methanol. For the GC-MS analysis of urocanic acid, samples were prepared by HPLC fractionation and derivatized with MSTFA, as described above. To enable the analysis of β-Tyr formation, MeOH was added, the samples were centrifuged, and then the solvent was removed completely by evaporation. The resulting residue was dissolved in borate buffer, and then the amino acids were derivatized, as described above.

Site-directed mutagenesis of CmdF: An overlap extension PCR strategy with Phusion polymerase was employed to create mutations or deletions in the *cmdF* sequence.[34] Vector-specific primers, pGEX-up and pGEX-down, were used in combination with primers binding at the respective complementary strand, which exhibit an overlap containing the desired mutation (Table S2). The plasmid pGEX-TAM was used as a template.[7] In a first round of PCR, two overlapping fragments were amplified separately and gel purified, and then the fragments were used as templates for a second round of PCR with primers pGEX-up and pGEX-down to amplify the mutated coding sequence with flanking BamHI and EcoRI restriction sites. The obtained ≈1.6 kbp fragments were digested accordingly and ligated into the BamHI/EcoRI digested pGEX-6P-1 vector backbone, followed by the transformation of the vector into *E. coli* DH10B. The presence of the introduced mutations and absence of undesired secondary mutations in the resulting plasmids were confirmed by sequencing.

Acknowledgements

The authors wish to thank Kira J. Weissman for critical reading of the manuscript and helpful discussion and Heinrich Steinmetz (Helmholtz Centre for Infection Research, Braunschweig, Germany) for kindly providing myxovalargin A. This work was funded by grants from Deutsche Forschungsgemeinschaft (DFG) and Bundesministerium für Bildung und Forschung (BMB + F) to R.M.

Keywords: amino acids · aminomutases · ammonia lyase · enzyme catalysis · stereoselectivity

[1] T. M. Zabriskie, J. A. Klocke, C. M. Ireland, A. H. Marcus, T. F. Molinski, D. J. Faulkner, C. Xu, J. Clardy, *J. Am. Chem. Soc.* **1986**, *108*, 3123–3124.
[2] B. Kunze, R. Jansen, H. Reichenbach, G. Höfle, *Liebigs Ann. Chem.* **1996**, 285–290.
[3] U. Eggert, R. Diestel, F. Sasse, R. Jansen, B. Kunze, M. Kalesse, *Angew. Chem.* **2008**, *120*, 6578–6582; *Angew. Chem. Int. Ed.* **2008**, *47*, 6478–6482.
[4] S. D. Christenson, W. Liu, M. D. Toney, B. Shen, *J. Am. Chem. Soc.* **2003**, *125*, 6062–6063.
[5] S. G. Van Lanen, T. J. Oh, W. Liu, E. Wendt-Pienkowski, B. Shen, *J. Am. Chem. Soc.* **2007**, *129*, 13082–13094.
[6] H. Steinmetz, H. Irschik, H. Reichenbach, G. Höfle in *Chemistry of Peptides and Proteins: Proceedings of the Sixth USSR–FRG Symposium on Chemistry of Peptides and Proteins, Hamburg, 1987* (Eds.: W. A. König, W. Voelter), Attempto, Tübingen, **1987**, pp. 13–18.
[7] S. Rachid, D. Krug, K. J. Weissman, R. Müller, *J. Biol. Chem.* **2007**, *282*, 21810–21817.
[8] S. Rachid, D. Krug, I. Kochems, B. Kunze, M. Scharfe, H. Blöcker, T. M. Zabriskie, R. Müller, *Chem. Biol.* **2006**, *13*, 667–681.
[9] L. Poppe, J. Rétey, *Angew. Chem.* **2005**, *117*, 3734–3754; *Angew. Chem. Int. Ed.* **2005**, *44*, 3668–3688.
[10] D. Röther, L. Poppe, S. Viergutz, B. Langer, J. Rétey, *Eur. J. Biochem.* **2001**, *268*, 6011–6019.
[11] C. V. Christianson, T. J. Montavon, G. M. Festin, H. A. Cooke, B. Shen, S. D. Bruner, *J. Am. Chem. Soc.* **2007**, *129*, 15744–15745.
[12] M. Langer, A. Pauling, J. Rétey, *Angew. Chem. Int. Ed. Engl.* **1995**, *34*, 1464–1465.
[13] A. C. Schroeder, S. Kumaran, L. M. Hicks, R. E. Cahoon, C. Halls, O. Yu, J. M. Jez, *Phytochemistry* **2008**, *69*, 1496–1506.
[14] L. Xiang, B. S. Moore, *J. Bacteriol.* **2005**, *187*, 4286–4289.
[15] M. C. Moffitt, G. V. Louie, M. E. Bowman, J. Pence, J. P. Noel, B. S. Moore, *Biochemistry* **2007**, *46*, 1004–1012.
[16] K. T. Watts, B. N. Mijts, P. C. Lee, A. J. Manning, C. Schmidt-Dannert, *Chem. Biol.* **2006**, *13*, 1317–1326.
[17] G. V. Louie, M. E. Bowman, M. C. Moffitt, T. J. Baiga, B. S. Moore, J. P. Noel, *Chem. Biol.* **2006**, *13*, 1327–1338.
[18] S. D. Christenson, W. Wu, M. A. Spies, B. Shen, M. D. Toney, *Biochemistry* **2003**, *42*, 12708–12718.
[19] H. D. Mootz, D. Schwarzer, M. A. Marahiel, *Proc. Natl. Acad. Sci. USA* **2000**, *97*, 5848–5853.
[20] J. A. Kyndt, T. E. Meyer, M. A. Cusanovich, J. J. Van Beeumen, *FEBS Lett.* **2002**, *512*, 240–244.
[21] H. Irschik, H. Reichenbach, *J. Antibiot.* **1985**, *38*, 1237–1245.
[22] G. A. O'Toole, R. Kolter, *Mol. Microbiol.* **1998**, *28*, 449–461.
[23] H. B. Bode, M. W. Ring, G. Schwär, M. O. Altmeyer, C. Kegler, I. R. Jose, M. Singer, R. Müller, *ChemBioChem* **2009**, *10*, 128–140.
[24] J. C. Calabrese, D. B. Jordan, A. Boodhoo, S. Sariaslani, T. Vannelli, *Biochemistry* **2004**, *43*, 11403–11416.
[25] C. V. Christianson, T. J. Montavon, S. G. Van Lanen, B. Shen, S. D. Bruner, *Biochemistry* **2007**, *46*, 7205–7214.
[26] D. Röther, L. Poppe, G. Morlock, S. Viergutz, J. Rétey, *Eur. J. Biochem.* **2002**, *269*, 3065–3075.
[27] M. Berner, D. Krug, C. Bihlmaier, A. Vente, R. Müller, A. Bechthold, *J. Bacteriol.* **2006**, *188*, 2666–2673.
[28] J. S. Williams, M. Thomas, D. J. Clarke, *Microbiology* **2005**, *151*, 2543–2550.
[29] M. B. Austin, P. E. O'Maille, J. P. Noel, *Nat. Chem. Biol.* **2008**, *4*, 217–222.
[30] L. Shimkets, M. Dworkin, H. Reichenbach in *The Prokaryotes, Vol. 7* (Ed.: M. Dworkin), Springer, Berlin, **2006**, pp. 31–115.
[31] R. H. Buck, K. Krummen, *J. Chromatogr.* **1987**, *387*, 255–265.
[32] P. Vandamme, T. Coenye, *Int. J. Syst. Evol. Microbiol.* **2004**, *54*, 2285–2289.
[33] K. Kashefi, P. L. Hartzell, *Mol. Microbiol.* **1995**, *15*, 483–494.
[34] S. N. Ho, H. D. Hunt, R. M. Horton, J. K. Pullen, L. R. Pease, *Gene* **1989**, *77*, 51–59.

Received: November 13, 2008
Published online on February 16, 2009

